

# Calculated optical properties of GaX (X = P, As, Sb) under hydrostatic pressure

Y. Al-Douri · Ali Hussain Reshak

Received: 12 January 2011 / Accepted: 7 April 2011  
© Springer-Verlag 2011

**Abstract** The hydrostatic pressure dependence of the principal energy gaps and of the optical properties of GaX (X = P, As and Sb) has been calculated using the full potential-linearized augmented plane wave (FP-LAPW) method. The generalized gradient approximation (GGA) for the exchange and correlation potential is applied. Also, we have used the Engel–Vosko GGA formalism, which optimizes the corresponding potential for band-structure and the optical properties calculations. Structural properties such as equilibrium lattice constants, the bulk modulus, and its pressure derivatives were calculated for GaP, GaAs, and GaSb in the zinc-blende structure (ZB). We have found that the results of the structural properties calculations are in agreement with those of ab initio and experimental data. In general, the pressure dependence of the principal energy gaps is compared to other values. The same is for the pressure coefficient. However, for the same structure, the comparison of our results with those of experimental and theoretical calculations shows good agreement. On the other hand, the effect of the applied pressure is clearly seen in

the optical properties especially near the energy transition regions.

## 1 Introduction

The most remarkable aspect of III–V compounds of tetrahedral coordinated structures is their low density. Therefore, under pressure, a tetrahedral coordinated semiconductor can be transformed to a structure with high density. In this field, the development of the diamond anvil cell [1] and its inherent ruby fluorescence monometer [2] have given a new impetus to studies of electronic and vibronic states of semiconductors under very high hydrostatic pressure [3, 4]. The transition from coordination number  $N_c = 4 \rightarrow 6$  is well demonstrated by the use of a computational method based on total-energy calculations [5–8].

The GaP, GaAs, and GaSb compounds in the zinc-blende structure (ZB) have the lowest minimum total energy. It is the most stable phase of these compounds at ambient pressure. When the pressure is applied, the volume decreases and a transition to the  $\beta$ -Sn (or NaCl) phase occur at relatively low pressure. This observation is interesting when one tries to gain some information about the many properties of the group of binary compounds under pressure.

There have been many electronic band structure calculations for III–V semiconductors. These include the empirical pseudopotential method (EPM) [9, 10], the tight binding (TB) [11, 12], full potential method [12, 19], and the pseudopotential total energy approach [13]. In the present work, we have reported the FP-LAPW calculations of the pressure dependence of the band structures in GaX (X = P, As and Sb) to study the structural, electronic, and optical properties. The exchange and correlation potential has been calculated using the generalized gradient approximation (GGA)

Y. Al-Douri (✉)  
Institute of Nano Electronic Engineering,  
University Malaysia Perlis, 01000 Kangar, Perlis, Malaysia  
e-mail: [yaldouri@yahoo.com](mailto:yaldouri@yahoo.com)  
Fax: +60-4-9798578

A.H. Reshak (✉)  
Institute of Physical Biology, South Bohemia University,  
Nove Hrady 37333, Czech Republic  
e-mail: [maalidph@yahoo.co.uk](mailto:maalidph@yahoo.co.uk)  
Fax: +420-386-361231

A.H. Reshak  
School of Materials Engineering,  
University Malaysia Perlis (UniMAP), P.O. Box 77,  
d/a Pejabat Pos Besar, 01000 Kangar, Perlis, Malaysia

[14] for the total energy calculations, in addition the Engel–Vosko GGA formalism [15], which optimizes the corresponding potential has been used for band-structure calculations to determine the pressure effects on the band gaps and for the optical properties. Because of their small energy gaps, this investigation concerns only the pressure below the phase transition. Our results have been compared to those of Bouarissa et al. [16], who employed the virtual crystal approximation into empirical pseudopotential method [17]. The comparison has also been made with recent calculations of Briki et al. [18], in addition to the FP-LAPW plus local orbitals calculations by Bouhemadou et al. [19].

The organization of this paper is as follows. In Sect. 2, we present the computational procedure. The Murnaghan equation of state and our main results of the FP-LAPW calculations regarding the structural, electronic and optical properties are devoted in Sect. 3. Also, in this section, special attention has been given to the pressure dependence of the investigated properties including the discussion and the comparison with other results (theoretical and experimental). Finally, we conclude our results in Sect. 4.

## 2 Theoretical approach

The calculations were carried out using the full potential linearized augmented plane wave (FP-LAPW) method as implemented in WIEN2K code [22]. In the FP-LAPW method, the unit cell is partitioned into non-overlapping muffin-tin spheres around the atomic sites and an interstitial region. Among these two types of regions, different basis sets are used; the Kohn–Sham equation which is based on the density functional theory (DFT) [23, 24] is solved in a self-consistent scheme. The exchange correlation potential was treated using the generalized gradient approximation (GGA) [14] in which the orbitals of Ga ( $3d^{10}4s^24p^1$ ), P ( $3s^23p^3$ ), As ( $3d^{10}4s^24p^3$ ), and Sb ( $4d^{10}5s^25p^3$ ) are treated as valence electrons for the total energy calculations. Also, we used the Engel–Vosko GGA (EVGGA) formalism [15] for band structure and optical properties calculations.

The crystal structure of these compounds is zincblende with two atoms per unit cell, the full space group is 216 (F-43m), which includes 24 symmetry operations and excludes inversion symmetry. In the calculation, 537 plane waves have been used for the expansion of the charge density and the potential in the interstitial region and lattice harmonics up to  $l = 8$  for the expansion inside the muffin-tin spheres. The muffin-tin radii were assumed to be 2.0 atomic units (a.u.) for Ga, P, As, and Sb. The dependence of the total energy on the number of  $k$  points in the irreducible wedge of the first Brillouin zone (BZ) has been explored within the linearized tetrahedron scheme [22] by performing the calculation for 10  $k$  points and extrapolating to an infinite number of  $k$  points. A satisfactory degree of convergence was

achieved by considering a number of FP-LAPW basis functions up to  $R_{MT}K_{\max} = 8$  (where  $R_{MT}$  is the average radius of the muffin-tin spheres and  $K_{\max}$  is the maximum value of the wave vector  $\mathbf{K} = \mathbf{k} + \mathbf{G}$ ). This corresponds, at the equilibrium lattice constant, to about 217 basis functions. In order to keep the same degree of convergence for all the studied lattice constants, we kept the values of the sphere radii and of  $K_{\max}$  constant over the whole range of lattice spacings. We also mention that the integrations in reciprocal space were performed using the special points method. A mesh of  $4 \times 4 \times 4$  which represents 100  $k$  points in the first Brillouin zone was used. This corresponds to ten special  $k$  points in the irreducible wedge for the zincblende structure. The ab initio calculation of the valence and conduction band energy eigenvalues has been performed at 111 points in the 1/48-th of the irreducible Brillouin zone (BZ).

## 3 Results and discussion

The theoretical lattice constants and bulk modulus are obtained through fitting the total energy data with the Murnaghan equation of state [20, 21]:

$$E(V) - E_0(V) = \frac{B_0 V}{B'_0} \left[ \frac{(V_0/V)^{B'_0}}{B'_0 - 1} + 1 \right] - \frac{B_0 V}{B'_0 - 1}, \quad (1)$$

where  $E(V)$  is the DFT ground-state energy with the cell volume  $V$ ,  $V_0$  is the unit-cell volume at zero pressure,  $B$  denotes the bulk modulus, and its first pressure derivative is  $B'_0 = \partial B / \partial P$  at  $P = 0$ .

The calculated structural properties (lattice constants  $a$ , bulk modulus  $B$ , and first derivative of bulk modulus  $B'_0$ ) of the GaP, GaAs, and GaSb binaries are summarized in Table 1. Our calculations show an overestimation in the lattice parameters and an underestimation in the bulk modulus in comparison to those of experiment (see Table 1), due to the use of the GGA. One can note that the lattice constants of these semiconductors increase with increase of the atomic number of the corresponding P, As, and Sb atoms. However, our calculated GGA values of the bulk modulus agree well with other calculations, but the values are smaller than the experimental ones. The overall calculated structural parameters by GGA follow the expected trend; the lattice constant is overestimated and the bulk modulus is underestimated.

Using our calculated values of the bulk modulus  $B_0$  and its first pressure derivatives  $B'$ , the appropriate equation [25] for calculating the volume changes with applied pressure is

$$p = \frac{B_0}{B'_0} \left[ \left( \frac{V_0}{V} \right)^{B'_0} - 1 \right], \quad (2)$$

where  $p$  is pressure.

**Table 1** The equilibrium calculated lattice constant  $a$ , bulk modulus  $B_0$ , and first pressure derivative  $B'$  correspond to experimental and theoretical ones

	$a$ (Å)	$B_0$ (GPa)	$B'$
GaP	5.50 <sup>a</sup> , 5.386 <sup>b</sup> , 5.451	77.21 <sup>a</sup> , 86.8 <sup>b</sup> , 88.7 <sup>b'</sup> , 83.98 <sup>c</sup> , 77.3 <sup>d</sup> , 76.51 <sup>e</sup> , 83.98 <sup>f</sup>	4.88 <sup>a</sup> , 4.00 <sup>b</sup> , 4.52 <sup>d</sup> , 4.30 <sup>e</sup>
GaAs	5.73 <sup>a</sup> , 5.601 <sup>b</sup> , 5.653 <sup>b'</sup>	60.83 <sup>a</sup> , 70.8 <sup>b</sup> , 74.8 <sup>b'</sup> , 72.45 <sup>c</sup> , 60.2 <sup>d</sup> , 72.45 <sup>f</sup>	4.60 <sup>a</sup> , 3.36 <sup>b</sup> , 5.20 <sup>d</sup>
GaSb	6.19 <sup>a</sup> , 6.032 <sup>b</sup> , 6.118 <sup>b'</sup>	45.92 <sup>a</sup> , 55.7 <sup>b</sup> , 57 <sup>b'</sup> , 55.48 <sup>c</sup> , 45.9 <sup>d</sup> , 55.48 <sup>f</sup>	5.16 <sup>a</sup> , 3.83 <sup>b</sup> , 4.16 <sup>d</sup>

a: This work; b & b': [5] Theo. & Exp., respectively; c: [25], d: [18], e: [19], f: [26]

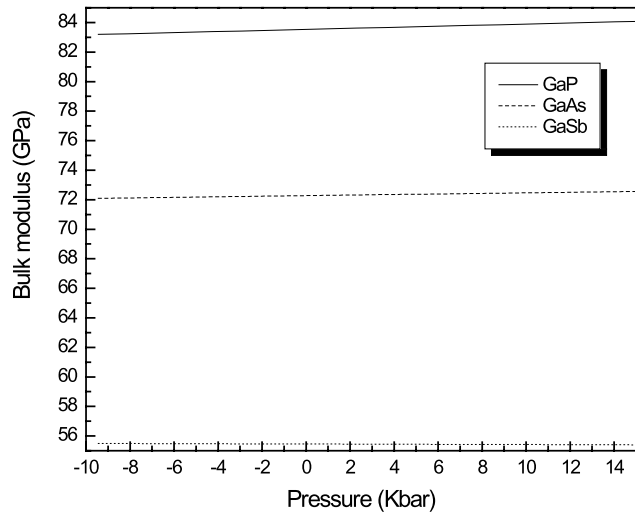


**Fig. 1** Fitted variation of the equilibrium bulk modulus versus hydrostatic pressure for GaP, GaAs, and GaSb

We have calculated the bulk modulus  $B_0$  of these compounds by using our calculated lattice constant. The computation of  $B_0$  was to test our model [26], where the well-known formula used is given as

$$B_0 = [3000 - \lambda 100] \left( \frac{a}{2} \right)^{-3.5} \quad (3)$$

where  $a$  is the lattice constant in (Å),  $\lambda$  is an empirical parameter which accounts for the effect of ionicity; 0, 1 and 2 for group-IV, III-V, and II-VI semiconductors, respectively. In Table 1, the calculated bulk modulus values are compared with experimental and theoretical values. We may conclude that the present bulk moduli calculated in different way are in good agreement with the experimental and theoretical ones. On the other hand, Fig. 1 exhibits the sensitive increasing variation of the pressure dependence of the bulk modulus for GaP and GaAs except for GaSb that shows a little bit of decreasing.

At normal pressure, the covalent semiconductors are four-fold coordinated. The reason that the density is so low is that nearest neighbors are bound by overlapping hybridized orbitals, which are the well-known  $sp^3$  hybrids with tetrahedral direction. Therefore, these covalent compounds

can be transformed either through chemical shifts or under pressure into a denser structure, which may be ionic or metallic. Thermodynamically, the three structures are separated by a first-order phase transition, but, microscopically, the responsibility of the interactions for the phase transition may be the same as for the chemical trends within the covalent structures.

Hence, to discuss the results of the electronic properties of these compounds, it is possible to tune the band gaps using pressure. The pressure dependence of principal energy gaps,  $E_g$  for the ZB phase is shown in Table 2, which indicates that the fundamental band gap changes to indirect for GaP, GaAs and GaSb. Comparisons of our calculated band gaps with other works are listed in Table 2, where we found an agreement between our results and those of others [11, 16, 18, 27–32]. Due to these small values, these compounds have been classified as narrow band gaps semiconductors. Because of their use in infrared light generation and detection, the band gap variations, especially under pressure, represent an important property to study. In contrast, the fundamental gaps for GaAs and GaSb become indirect (L) at pressures 13.277 and 9.710 Kbar, respectively. While for GaP, the fundamental gap becomes indirect (X) at 14.828 Kbar. Hence, the pressure values considered here are 14.828, 13.277, and 9.710 Kbar for GaP, GaAs, and GaSb, respectively. To see the quantitative changes, we are interested in the pressure dependence of the minimum band gaps. As mentioned in Table 2, the band gaps decrease at the L point for GaAs and GaSb, while it decreases at the X point for GaP when the pressure increases. These values decrease on going from GaP to GaAs till GaSb compounds. We have found these energy band gaps are 2.2, 1.85, and 1.15 eV for GaP, GaAs, and GaSb, respectively. From Fig. 2, we remark that the variation of band gaps versus pressure shows an increasing change for GaP, GaAs and GaSb. From these curves, we found that the values of the pressure coefficient of the minimum gap  $dE_g/dP$  are 8.85, 10.73, and 17.91 meV/bar for GaP, GaAs, and GaSb, respectively. Then our results are underestimated, coincided, and overestimated with increasing the atomic number of P, As, and Sb, respectively, compared to those of experimental [31] and theoretical [32] data.

**Table 2** Calculated lattice constant, direct and indirect energy gaps, gap between first and second valance band at X point and pressure coefficient of GaP, GaAs, and GaSb at ambient and under pressure effect correspond to other experimental and theoretical ones

$P$ (Kbar)	GaP			GaAs			GaSb			$dE_0/dP$ (meV/bar)	$E_g\Gamma\Gamma$	$E_g\Gamma X$	$E_g(2-1)X$				
	$a$ (Å)	$E_{g\Gamma\Gamma}$	$E_{g\Gamma X}$	$E_{g(2-1)X}$	$P$ (Kbar)	$a$ (Å)	$E_{g\Gamma\Gamma}$	$E_{g\Gamma X}$	$E_{g(2-1)X}$								
0.0	5.501 <sup>a</sup>	2.0 <sup>a</sup>	2.50 <sup>a</sup>	2.09 <sup>a</sup>	3.1	0.0	5.733 <sup>a</sup>	0.49 <sup>a</sup>	2.40 <sup>a</sup>	1.3 <sup>a</sup>	2.2	0.0	6.193 <sup>a</sup>	0.4 <sup>a</sup>	1.60 <sup>a</sup>	0.8 <sup>a</sup>	2.3
5.451 <sup>b</sup>	2.774 <sup>b</sup>	2.25 <sup>b</sup>	2.6 <sup>b</sup>				5.653 <sup>b</sup>	1.42 <sup>b</sup>	1.81 <sup>b</sup>	1.72 <sup>b</sup>			6.118 <sup>b</sup>	0.715 <sup>b</sup>	1.012 <sup>b</sup>	0.777 <sup>b</sup>	
5.52 <sup>b</sup>	2.78 <sup>c</sup>	2.26 <sup>c</sup>	2.6 <sup>c</sup>				5.75 <sup>b</sup>	1.42 <sup>d</sup>	1.81 <sup>d</sup>	1.72 <sup>d</sup>			6.22 <sup>b</sup>	0.725 <sup>e</sup>	1.03 <sup>f</sup>	0.761 <sup>f</sup>	
2.88 <sup>g</sup>	2.35 <sup>g</sup>	2.739 <sup>g</sup>					1.419 <sup>g</sup>	1.95 <sup>g</sup>	1.729 <sup>g</sup>				0.72 <sup>g</sup>	1.02 <sup>g</sup>	0.769 <sup>g</sup>		
1.46 <sup>h</sup>	1.68 <sup>h</sup>	1.51 <sup>h</sup>					0.05 <sup>h</sup>	1.49 <sup>h</sup>	0.79 <sup>h</sup>				-0.35 <sup>h</sup>	0.94 <sup>h</sup>	0.28 <sup>h</sup>		
1.45 <sup>k</sup>							0.4 <sup>k</sup>	0.4 <sup>k</sup>					0.2 <sup>k</sup>				
14.828	5.503	3.15	2.2	2.6	1.6	13.277	5.739	1.98	2.05	1.85	5.3	9.710	1.195	1.25	1.40	1.15	1.05
$dE_0/dP$ (meV/bar)	8.85 <sup>a</sup>	10.7 <sup>i</sup>	9.7 <sup>j</sup>				10.73 <sup>a</sup>	10.73 <sup>i</sup>	10.73 <sup>j</sup>				17.91 <sup>a</sup>	14.7 <sup>i</sup>	13.8 <sup>j</sup>		

a: This work; b: [16] EPM; c: [27] exp.; d: [28] exp.; e: [29] exp.; f: [30] exp.; g: [11] TB; h: [18] FP-LAPW; i: [31] exp.; j: [32]; k: [12] FP-LAPW&LMTO

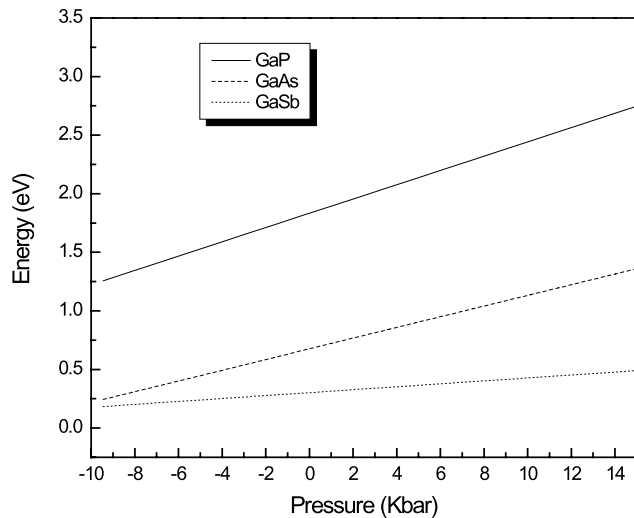


**Fig. 2** Fitted variation of the equilibrium energy gap versus hydrostatic pressure for GaP, GaAs and GaSb

In order to test the validity of our recent model [33], we have carried out this calculation to GaP, GaAs and GaSb compounds using heteropolar gap, hence we have calculated the ionicity character  $f_i$ . The computation of  $f_i$  is trivial and the accuracy of the results reaches to that of the ab initio calculation. We have used the formula [33]

$$f_i = \left[ \left( \frac{E_g}{E_g - 1} \right)^{-1} - 0.75 \right] - \left[ \left( \frac{1}{E_g} \right) - 0.66 \right], \quad (4)$$

where  $E_g$  is the energy gap between the first and the second valence band at point X and 1 is equal to 1 eV. The calculated ionicity values are compared with Phillips [34], Garcia and Cohen [35], and Cristensen et al. [36]. The comparison is given in Table 3. The variation of ionicity versus hydrostatic pressure is displayed in Fig. 3. It is clearly seen that the ionicity character under pressure effect decreases continuously except for GaAs as an indication of the structural phase transition to  $\beta$ -Sn phase [7].

It is a good notice to mention that the critical pressure is the value that separates the decrease and the increase of the ionicity value. The change of the ionicity factor under pressure is confirmed by changing the energy gap values as shown in Table 2. As a consequence, a fluctuation of the ionicity factor appears. This result shows that the calculated ionicity values exhibit the same chemical trends as those found in the values derived by Phillips [34] and in accordance with the results of others [35, 36].

The optical properties of solids can be described in terms of the optical dielectric function. Previous results have been reported experimentally [37, 38, 42–44] and theoretically [12, 39, 40], they have been measured and calculated the absorption [37], imaginary part of the optical dielectric function [12, 38, 39, 42], reflectivity [12, 43, 44] and the refrac-

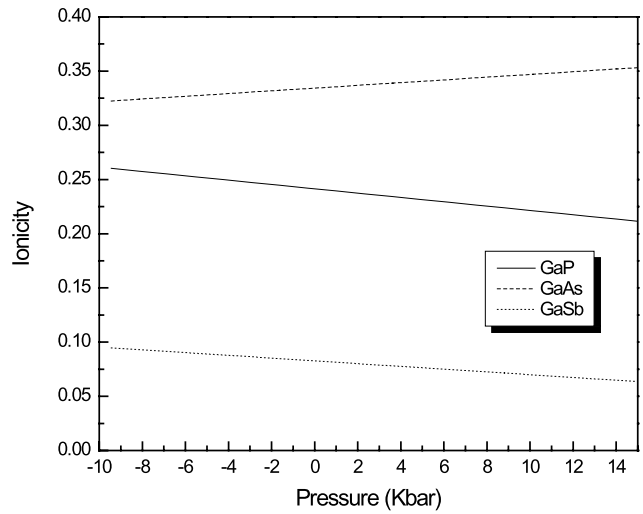


**Fig. 3** Fitted variation of the ionicity factor versus hydrostatic pressure for GaP, GaAs, and GaSb

**Table 3** Ionicity factor values for GaP, GaAs and GaSb correspond to other experimental and theoretical ones at ambient pressure and under pressure effect

	$f_i$ at 0 Kbar	$f_i$	$f_i$ under pressure
GaP	0.264 <sup>a</sup>	0.327 <sup>b</sup>	0.384\$
		0.371 <sup>c</sup>	0.361 <sup>d</sup>
GaAs	0.321 <sup>a</sup>	0.310 <sup>b</sup>	0.264+
		0.316 <sup>c</sup>	0.310 <sup>d</sup>
GaSb	0.083 <sup>a</sup>	0.261 <sup>b</sup>	0.030#
		0.169 <sup>c</sup>	0.108 <sup>d</sup>

a: This work; b: [34], c: [35], d: [36]. \$: under 14.828 Kbar, +: under 13.277 Kbar, #: under 9.710 Kbar

tive index [40], respectively. In this work, we have calculated the imaginary part and its dependences on pressure for the three compounds. Figure 4 illustrates the calculated imaginary part of the optical dielectric function and its dependences on pressure for the GaP, GaAs, and GaSb along with the experimental data [42]. Our calculation shows that the dispersion of the imaginary part of the frequency dependent dielectric function at ambient pressure (0 Kbar) for GaP and GaAs agree well with the experimental data in the matter of peak positions but it shows less magnitude than the experimental data. While in GaSb the first theoretical peak shifted by around 0.5 eV toward higher energies. For the high pressure phase, all the investigated compounds show good agreement in the matter of the peak position and heights. From a quantitative point of view, the imaginary part of these compounds is similar with minor differences.

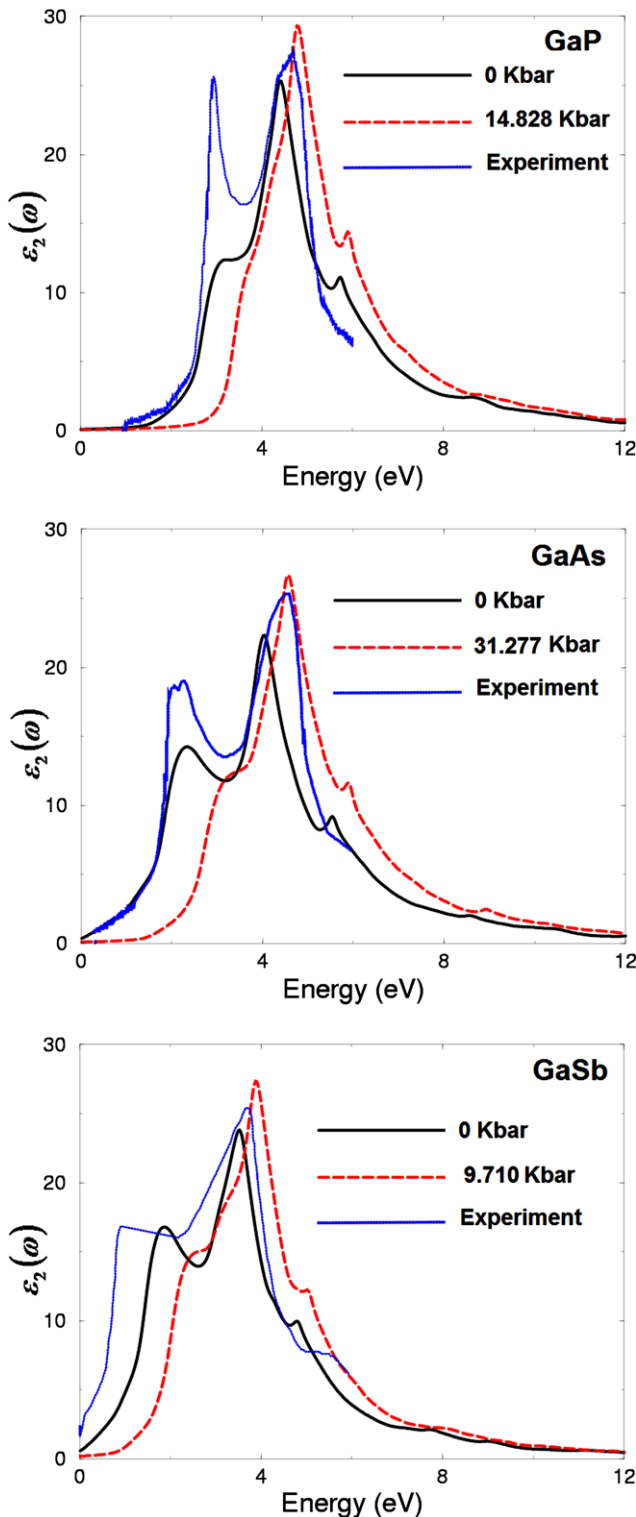


**Fig. 4** Imaginary part of the dielectric function of GaP, GaAs, and GaSb (solid line at ambient pressure and dash line under pressure) along with the experimental data [42]

Following these figures, one can note that there is one main peak situated between two small humps. When we apply the pressure, we observed that there is no change in the struc-

ture of the main peak just it shifts toward higher energies by around 1.0 eV with increasing the amplitude. Whereas the left hump shows dramatic change with applying the pressure and keeping the right hump at the same position just with higher amplitude. To explain the behavior of the left hump under the pressure, one needs to look at the optical transition matrix elements. We found that this behavior is attributed to the fact that applying high pressure causes to push the valence bands (VB) towards lower energies and the conduction band minimum (CBM) toward higher energies resulting in changing the energy band gap from direct to indirect one with increasing the value of the energy band gap. That causes to change the optical transitions between the top of valence band and bottom of conduction band from direct to indirect optical transitions. These behaviors remain valid for all the pressures listed in Table 2. This is the reason why we have considered only the critical values of the pressures before any phase transition.

From the imaginary part of the dielectric function, the real part was calculated (not shown here) using Kramers–Kronig relations [41]. Using the calculated dispersions of imaginary and real parts of the dielectric function, one can evaluate other optical properties such as absorption coefficients  $I(\omega)$ , the conductivity  $\sigma(\omega)$ , reflectivity spectra  $R(\omega)$  and the refractive indices  $n(\omega)$ . We show these quantities in Figs. 5 and 6, respectively.

In Fig. 6, we show the reflectivity spectra along with the experimental data [43, 44] for GaP, GaAs, and GaSb compounds at ambient and under hydrostatic pressure. We should emphasize that our calculated reflectivity show good agreement with the experimental data in the matter of the peaks position and peaks height. It is interesting that there is an abrupt reduction in the reflectivity spectrum between 12.0 to 13.0 eV for both ambient and high pressure curves confirming the occurrence of a collective plasmon resonance. The depth of the plasmon minimum is determined by the imaginary part of the dielectric function at the plasma resonance and is representative of the degree of overlap between the inter-band absorption regions. The calculated absorption coefficient dispersion  $I(\omega)$  is shown in Fig. 5. At low energies between 0.0 to 4.0 eV and at higher energies (at around 13.0 eV), this crystal shows a fast increasing absorption. The calculated refractive index dispersions  $n(\omega)$  are shown in Fig. 6. We note that at low energy these compounds shows high refractive indices, which decrease at higher energies.

The calculated optical conductivity dispersion  $\sigma(\omega)$  for the investigated compounds at ambient and under hydrostatic pressure are shown in Fig. 5. The optical conductivity (OC) is related to the frequency-dependent dielectric function  $\epsilon(\omega)$  as  $\epsilon(\omega) = 1 + \frac{4\pi i \sigma(\omega)}{\omega}$ . The peaks in the optical conductivity spectra are determined by the electric-dipole transitions between the occupied states to the unoccupied states.

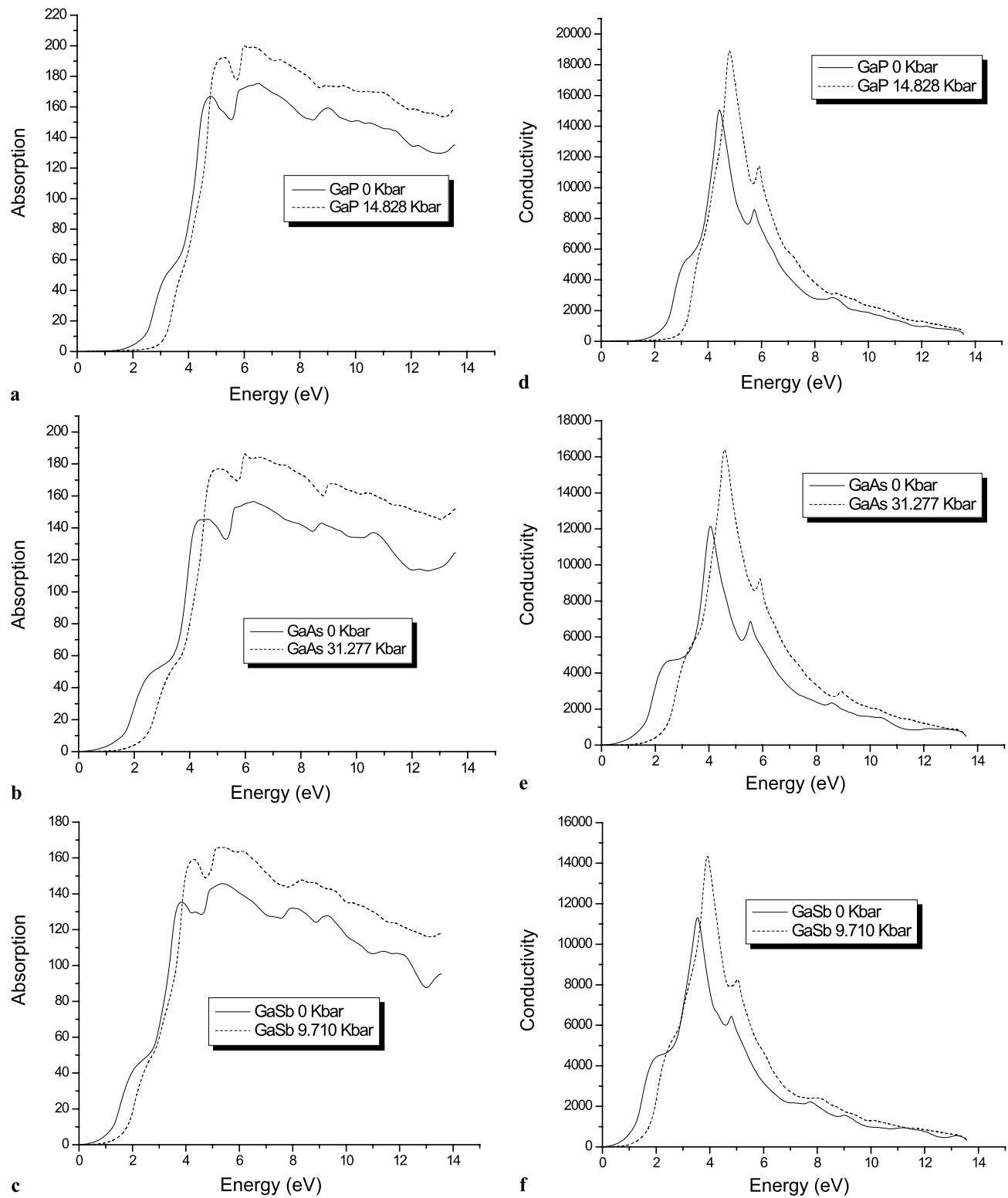


**Fig. 5** (a–c) Absorption and (d–f) conductivity of GaP, GaAs, and GaSb (*solid line* at ambient pressure and *dash line* under pressure)

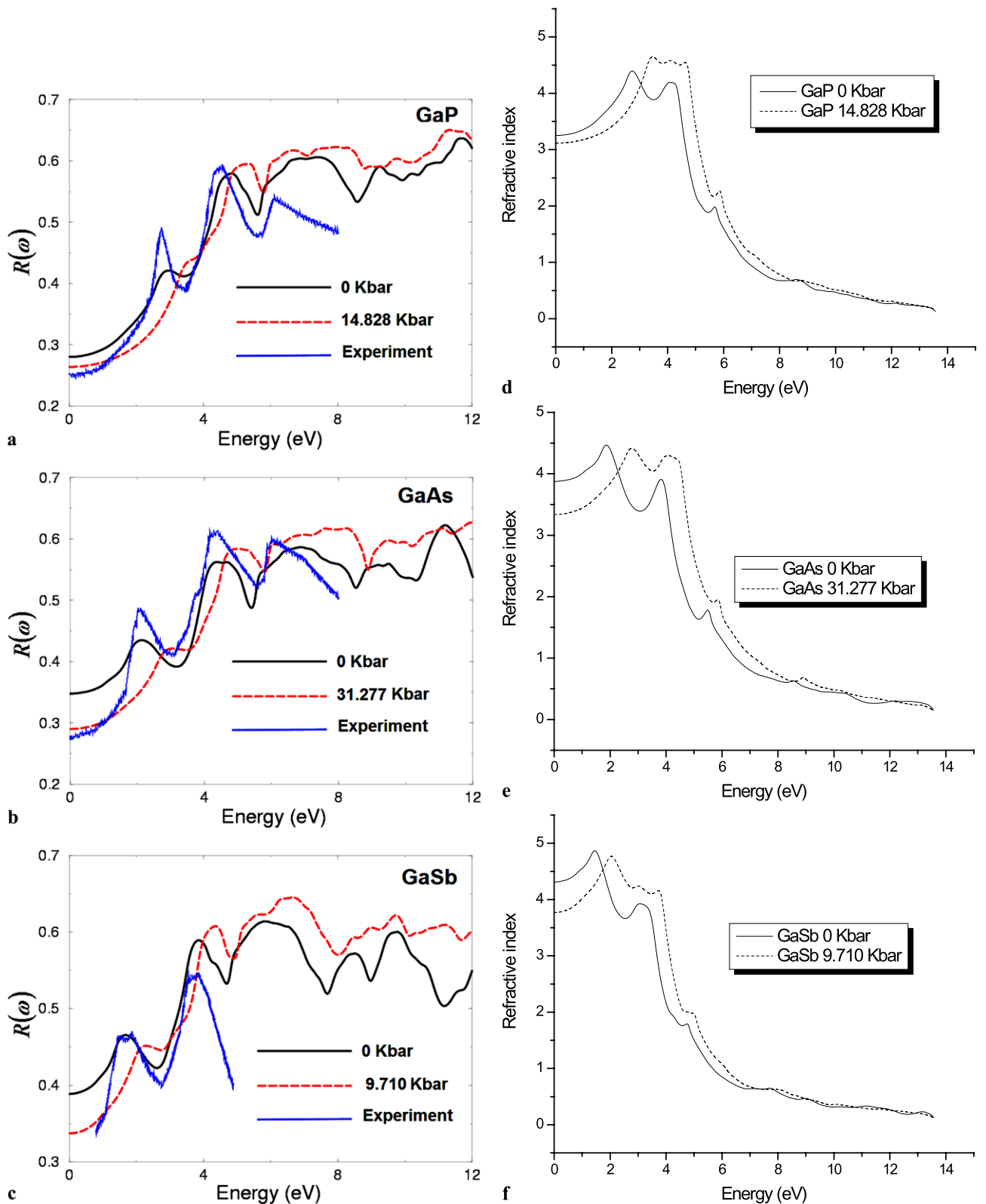


**Fig. 6** (a-c) Reflectivity along with the experimental data [43, 44], (d-f) refractive index of GaP, GaAs, and GaSb (*solid line* at ambient pressure and *dash line* under pressure)

## 4 Conclusion

In this work, we have reported the FP-LAPW calculations within the generalized gradient approximation (GGA) and Engel-Vosko GGA formalism for the exchange and correlation, to determine the structural, electronic and optical properties of the three GaP, GaAs and GaSb compounds at ambient and under pressure effect. The results show that the characteristics of the electronic properties under pressure are changed which is an indication of phase transformation to  $\beta$ -Sn phase. However, the pressure coefficient of the fundamental gap is in good agreement with other values. Although the calculated bulk moduli parameters are underestimated by GGA, the latter could be used to study the pressure dependence of the band gaps.

We have calculated the complex optical dielectric functions dispersion at ambient and under hydrostatic pressure. The spectral features of optical dielectric functions are discussed and analyzed using the optical transition matrix elements and the calculated band structure. We have compared our calculated results with the previous ones, and good agreement was found.

**Acknowledgements** This work has been achieved using FRGS grants numbered: 9003-00249 & 9003-00255. The author (Y.A.) would like to acknowledge MOSTI, Malaysia of BGM Program. In addition, thanks are due to TWAS-Italy, for full support of his visit to JUST-Jordan under TWAS-UNESCO Associateship.

For the author (A.H.R.), this work was supported from the institutional research concept of the Institute of Physical Biology, UFB (No. MSM6007665808), the program RDI of the Czech Republic, the project CENAKVA (No. CZ.1.05/2.1.00/01.0024), the grant No. 152/2010/Z of the Grant Agency of the University of South Bohemia. School of Materials Engineering, University Malaysia Perlis (UniMAP), P.O. Box 77, d/a Pejabat Pos Besar, 01000 Kangar, Perlis, Malaysia.

## References

- M.D. Frogley, J.L. Sly, D.J. Dunstan, Phys. Rev. B **58**, 12579 (1998)
- D. Boulanger, R. Parrot, Phys. Rev. B **66**, 205201 (2002)
- T. Hattori, K. Tsuji, Y. Miyata, T. Sugahara, F. Shimojo, Phys. Rev. B **76**, 144206 (2007)
- J. Serrano, A. Rubio, E. Hernández, A. Muñoz, A. Mujica, Phys. Rev. B **62**, 16612 (2000)
- S.B. Zhang, M.L. Cohen, Phys. Rev. B **35**, 7604 (1987)
- T. Soma, H.M. Kagaya, Solid State Commun. **50**, 1011 (1984)
- J.R. Chelikowsky, Phys. Rev. B **35**, 1174 (1987)
- Y.K. Vohra, S.T. Weir, A. Ruoff, Phys. Rev. B **31**, 7344 (1985)
- Y. Al-Douri, H. Aourag, Physica B **324**, 173 (2002)
- Y. Al-Douri, S. Mecabih, N. Benosman, H. Aourag, Physica B **325**, 362 (2003)
- M. Rabah, Y. Al-Douri, M. Sehil, D. Rached, Mater. Chem. Phys. **80**, 34 (2003)
- A.H. Reshak, Eur. Phys. J. B **47**, 503 (2005)
- S. Froyen, M.R. Cohen, Phys. Rev. B **28**, 3258 (1983)
- J.P. Perdew, S. Burke, M. Ernzerhof, Phys. Rev. Lett. **77**, 3865 (1996)
- E. Engel, S.H. Vosko, Phys. Rev. B **47**, 13164 (1993)
- N. Bouarissa, H. Baaziz, Z. Charifi, Phys. Status Solidi (b). Basic Solid State Phys. **231**, 403 (2002)
- M.L. Cohen, T.K. Bergstresser, Phys. Rev. **141**, 789 (1966)
- M. Briki, M. Abdelouhab, A. Zaoui, M. Ferhat, Superlattices Microstruct. **45**, 80 (2009)
- A. Bouhemadou, R. Khenata, M. Kharoubi, T. Seddik, Ali H. Reshak, Y. Al-Douri, Comput. Mater. Sci. **45**, 474 (2009)
- F.D. Murnaghan, Proc. Natl. Acad. Sci. USA **30**, 244 (1947)
- J.R. Macdonald, D.R. Powell, J. Res. Natl. Bur. Stand., A Phys. Chem. **75**, 441 (1971)
- P. Blaha, K. Schwarz, G.K.H. Madsen, D. Kvasnicka, J. Luitz, WIEN2K. Techn. Universität, Wien, Austria (2001). ISBN 3-9501031-1-1-2
- P. Hohenberg, W. Kohn, Phys. Rev. **136**, 864 (1964)
- W. Kohn, L.J. Sham, Phys. Rev. **140**, A1133 (1965)
- S. Berrah, H. Abid, A. Boukortt, M. Sehil, Turk. J. Phys. **30**, 513 (2006)
- Y. Al-Douri, H. Abid, H. Aourag, Mater. Chem. Phys. **87**, 14 (2004)
- M. Levinshtein, S. Rumyantsev, M. Shur (eds.), *Handbook Series on Semiconductor Parameters*, Vol. 1 (World Scientific, Singapore, 1996)
- D.E. Aspnes, C.G. Olson, D.W. Lynch, Phys. Rev. Lett. **37**, 766 (1976)
- S. Zollner, M. Garriga, J. Humlcek, S. Gopalan, M. Cardona, Phys. Rev. B **43**, 4349 (1991)
- C. Alibert, A. Joullie, A.M. Joullie, C. Ance, Phys. Rev. B **27**, 4946 (1983)
- T.S. Moss, *Handbook on Semiconductors*, vol. 2 (North-Holland, Amsterdam, 1980)
- M.D. Frogley, J.L. Sly, D.J. Dunstan, Phys. Rev. B **58**, 12579 (1998)
- Y. Al-Douri, H. Abid, A. Zaoui, H. Aourag, Physica B **301**, 295 (2001)
- J.C. Phillips, *Bonds and Bands in Semiconductors* (Academic Press, San Diego, 1973)
- A. Garcia, M.L. Cohen, Phys. Rev. B **47**, 4215 (1993)
- N.E. Christensen, S. Staphany, Z. Pawlowska, Phys. Rev. B **36**, 1032 (1987)
- A. Onton, J. Lumin. **7**, 95 (1973)
- A. Gheorghiu, M.-L. Theye, J. Non-Cryst. Solids **35** & **36**, 397 (1980)
- L. Wang, X. Chena, W. Lua, Y. Huang, J. Zhaob, Solid State Commun. **149**, 638 (2009)
- M. Linnik, A. Christou, Physica B **318**, 140 (2002)
- H. Tributsch, Z. Naturforsch. A, J. Phys. Sci. **32**, 972 (1977)
- D.E. Aspnes, A.A. Studna, Phys. Rev. B **27**, 985 (1983)
- H.R. Philipp, H. Ehrenreich, Phys. Rev. **129**, 1550 (1963)
- S.S. Vishnubhatla, J.C. Woolley, Can. J. Phys. **46**, 1769 (1968)